Surface studies of polypeptidic block copolymers by electron spectroscopy for chemical analysis: Poly(N^{ε}-trifluoroacetyl-L-lysine)–polysarcosine diblock copolymers

M. Gervais,* A. Douy and B. Gallot
Centre de Biophysique Moléculaire, C.N.R.S., 1A avenue de la Recherche Scientifique, 45071 Orleans Cedex 2, France

and R. Erre
Centre de Recherche sur les Solides à Organisation Cristalline Imparfaite, C.N.R.S., 1B rue de la Férollerie, 45071 Orleans Cedex 2, France
(Received 30 October 1985)

The surface of poly(N^{ε}-trifluoroacetyl-L-lysine)–polysarcosine (Kt.Sa) block copolymers was studied by electron spectroscopy for chemical analysis (e.s.c.a.) on films cast from methanol. The e.s.c.a. results indicate that the copolymer composition of the surfaces (e.g. outermost ~35 Å) may be significantly different from the overall bulk composition. A surface excess of Kt is observed for copolymers containing less than about 45 mol% Kt; the Kt excess increases as the bulk content of Kt decreases. Angular-dependent studies show that the concentration of Kt increases as the air–copolymer interface is approached. X-ray diffraction studies of the Kt.Sa copolymers in concentrated solution in methanol and in the dry state show that they exhibit a lamellar structure. Knowledge of this structure makes it easier to interpret the e.s.c.a. results. A model of the surface topography is proposed, namely that the lamellar structure is perpendicular to the air–polymer interface and the Kt domains are elevated above the Sa domains.

(Keywords: block copolymers; polypeptides; mesophases; electron spectroscopy for chemical analysis; X-ray diffraction)

INTRODUCTION

Surfaces of synthetic polymers which have microphase separated structures often show good blood compatibility. The biocompatibility of such polymer surfaces was shown to be greatly influenced by the shape and size of the microdomains[1], by their morphology[2,3] and by the balance between their hydrophobicity and their hydrophilicity[4,5]. Electron spectroscopy for chemical analysis (e.s.c.a.) was shown to be a valuable technique to obtain detailed information about the composition and the structure of the copolymer surfaces[6-17]. E.s.c.a. studies have revealed significant differences between the surface and the bulk composition of block copolymers. Polystyrene was found in excess at the surface of polystyrene–poly(ethylene oxide) block copolymers[9,10]. Polysiloxane was found in excess at the surface of the polystyrene–poly(dimethylsiloxane) block copolymers[12], of polycarbonate–poly(dimethylsiloxane) block copolymers[13] and of poly(propylene glycol)-poly(glycidoxypropylmethyl siloxane) networks[14]. Polybutadiene was found in excess at the surface of block copolymers with polybutadiene and poly(N^{ε}-benzyloxycarbonyl-L-lysine)[17]. These results are consistent with the view that the polymer chains of lower surface free energy will preferentially aggregate at the surface of phase-separated block copolymers.

E.s.c.a. was used to investigate the surface of poly(N^{ε}-trifluoroacetyl-L-lysine)–polysarcosine block copolymers.

Poly(N^{ε}-trifluoroacetyl-L-lysine)–polysarcosine 'Kt.Sa) block copolymers formed by a hydrophobic block of poly(N^{ε}-trifluoroacetyl-L-lysine) (Kt) and a hydrophilic block of polysarcosine (Sa) exhibit mesophases in the presence of water[18], a preferential solvent of the Sa blocks, and in the presence of methanol (MeOH), a mutual solvent of the Kt and Sa blocks.

In this paper we first describe briefly the structural study by X-ray diffraction of the mesophases exhibited by the Kt.Sa block copolymers in concentrated MeOH solutions and of the dry copolymers obtained after slow evaporation of MeOH. Then we report the results of e.s.c.a. studies on methanol-cast films of Kt.Sa block copolymers.

From the study of copolymers with different bulk compositions is derived the influence of the bulk composition of the copolymers on their surface composition.

Knowledge of the bulk structure determined by X-ray diffraction together with the measure of the angular dependence of the e.s.c.a. spectra has enabled us to propose a model for the topography of the Kt.Sa copolymers at the air–polymer interface.

EXPERIMENTAL

Material

The details of the synthesis and characterization of Kt.Sa diblock copolymers are described in a preceding

* To whom correspondence should be addressed

0032-3861/86/091513-08$03.00

paper[18]. The bulk compositions and number-average molecular weights are shown in *Table 1*.

Sample preparation

For X-ray diffraction analysis, mesomorphic gels were prepared by dissolution in a small excess of solvent. After homogenization the desired concentrations were obtained by slow evaporation of the solvent.

For e.s.c.a. analysis the Kt.Sa copolymers, and the Kt and Sa homopolymers were studied as thin films prepared by dip coating from dilute solution onto a flat nickel support. Thick coatings were obtained by multiple dipping to ensure the substrate Ni core level signals were no longer observable. These films were dried *in vacuo* for 24 h before use.

Methods

X-ray diffraction measurements were performed with a Guinier-type focusing camera using monochromator X-rays ($CuK\alpha_1$) and operating under vacuum.

E.s.c.a. spectra were recorded on a VG Escalab MKII spectrometer by using $MgK\alpha_{1,2}$ exciting radiation (1253.6 eV) from an X-ray tube operating at 10 kV and 10 mA. The base pressure in the measurement chamber was $\sim 5 \times 10^{-11}$ mbar.

Under the experimental conditions employed, the $Ag(3d_{5/2})$ line had a full width at half-maximum (*FWHM*) of 1.2 eV and a binding energy of 367.9 eV. The C_{1s} core level of the saturated hydrocarbon at 285.0 eV was used as an energy calibration. No smoothing procedure was used to modify the measured spectra. Spectra were resolved by computer calculation. A non-linear background was subtracted. The lineshapes of individual peaks were fitted to Gaussian spectral line functions. Binding energies are quoted to ± 0.2 eV and area ratios to $\pm 6\%$.

During the analysis time, samples were cooled to the temperature of liquid nitrogen.

To check the influence of the X-ray exposure time on the spectra, Kt and Sa samples were studied at several exposure times. The Kt spectrum shows modifications after more than 90 min so that the exposure time was limited to 60 min.

RESULTS AND DISCUSSION

Structure of copolymers

Block copolymers with a hydrophobic Kt block and a hydrophilic Sa block were shown to exhibit a periodic lamellar structure in the presence of MeOH, a mutual solvent of the two components, and in the dry state after evaporation of the solvent at a slow rate.

For solvent concentrations lower than about 40%:

(a) low-angle X-ray patterns of Kt.Sa copolymers display a set of sharp lines with Bragg spacings in the ratio 1:2:3 characteristic of a layered structure;

(b) wide-angle X-ray patterns of Kt.Sa copolymers and Kt homopolymer display a set of three sharp lines with Bragg spacings in the ratio $1:\sqrt{3}:\sqrt{4}$ characteristic of an hexagonal packing of the chains of Kt; and

(c) the α-helix type conformation of the Kt chains was inferred from these X-ray patterns[18] and from infra-red spectroscopy (bands amide I and amide II at 1655 and 1545 cm^{-1} respectively).

Table 1 Average molecular weights and bulk compositions for the three Kt.Sa diblock copolymers

	$\bar{M}_n \times 10^{-3}$		Bulk composition	
Sample	Kt	Sa	Wt% Kt	Mol% Kt
25	14.1	36.9	27.7	10.9
21	14.1	10.5	57.4	30.0
26	14.1	4.85	74.4	48.0

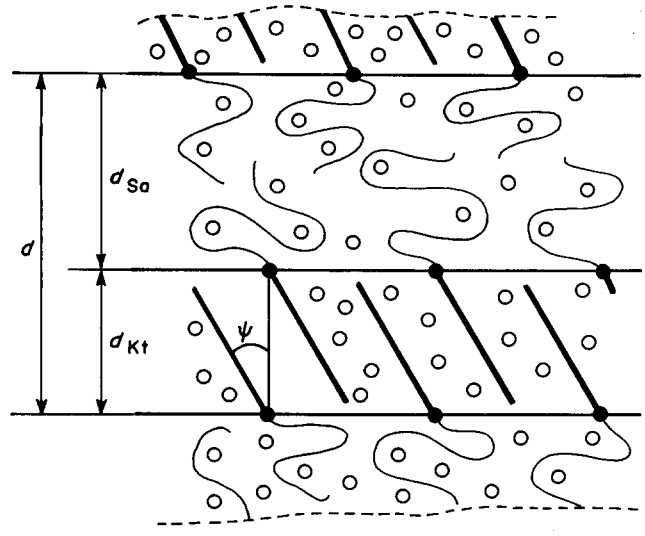

Figure 1 Schematic representation of the lamellar structure displayed by the Kt.Sa copolymers. The symbols are as follows: d, intersheet spacing; d_{Sa}, thickness of the layer containing the Sa chains; d_{Kt}, thickness of the layer containing the Kt chains; ψ, angle of tilt of the Kt chains

The lamellar structure results from the superposition of plane, parallel equidistant sheets; each elementary sheet of thickness d consists of two layers. One layer of thickness d_{Sa} contains the Sa chains in a disordered configuration and a part of the solvent. The other layer of thickness d_{Kt} contains the Kt chains in an α-helix type conformation and the other part of the solvent (*Figure 1*). The total thickness d of a sheet ($d = d_{Sa} + d_{Kt}$) is given directly by the Bragg spacings on the X-ray patterns.

The thicknesses d_{Kt} and d_{Sa} and the average surface S available for a molecule at the layer interface are calculated by formulae (1) and (2) based on simple geometrical considerations:

$$d_{Kt} = d\left(1 + \frac{CX_{Sa}V_{Sa} + (1-C)\phi_{Sa}V_S}{CX_{Kt}V_{Kt} + (1-C)\phi_{Kt}V_S}\right)^{-1} \quad (1)$$

$$S = \frac{2M_{Kt}V_{Kt}}{N_A d_{Kt}} \quad (2)$$

where C is copolymer concentration given by

$$C = \frac{\text{weight of copolymer}}{\text{weight of (copolymer + solvent)}}$$

X_{Sa} is weight fraction of the Sa block in the copolymer, X_{Kt} is weight fraction of the Kt block in the copolymer, V_{Sa} is specific volume of the Sa block ($V_{Sa} = 0.76\ cm^3\ g^{-1}$), V_{Kt} is specific volume of the Kt block ($V_{Kt} = 0.705\ cm^3\ g^{-1}$), V_S is specific volume of the solvent, ϕ_{Sa} and ϕ_{Kt} are partition coefficients of the solvent

($\phi_{Sa}+\phi_{Kt}=1$), M_{Kt} is number-average molecular weight of the Kt block, and N_A is Avogadro's number. The lattice parameter D of the hexagonal array formed by the Kt chains, namely the spacing between the axis of two neighbouring α-helices, is directly deduced from wide-angle X-ray patterns. The variation of D with the MeOH concentration is shown in *Figure 2* for the copolymer Kt.Sa 21.

Comparison of the values of D obtained for the system Kt homopolymer/MeOH and for the system Kt.Sa/MeOH has allowed us to determine the partition coefficients of the solvent. It was found that $\phi_{Sa}=0.60$ and $\phi_{Kt}=0.40$.

An example of the variation of the lamellar structure parameters with solvent concentration is illustrated in *Figure 3* for the copolymer Kt.Sa 21.

As the concentration of MeOH increases:

(a) the total thickness d of the sheet increases,

(b) the thickness d_{Sa} of the layer containing the Sa blocks increases,

(c) the thickness d_{Kt} of the layer containing the Kt blocks decreases, and

(d) the average surface S available for a molecule at the interface of the layers increases.

The decrease of the thickness d_{Kt} as the MeOH concentration increases was explained by demonstrating that the axes of the helices of the Kt chains are tilted on the plane of the lamellae[18] (*Figure 1*). The angle of tilt ψ, defined as the angle between the axis of the Kt helices and the normal to the interface, increases with solvent concentration (*Figure 3*). The geometrical parameters of the lamellar structure obtained for the copolymers after complete evaporation of MeOH were found to be equal to those obtained after complete evaporation of water[18].

Structural parameters for dried copolymers are listed in *Table 2*. As the Sa content of the copolymers decreases:

(a) the total thickness d of the sheet and the thickness d_{Sa} decrease,

(b) the thickness d_{Kt} increases,

(c) the specific surface S decreases, and

(d) the angle of tilt ψ of the Kt chains decreases so as to occupy the surface S available.

Surface composition

Composition determination. E.s.c.a. is based upon the kinetic analysis of photoelectrons ejected by the interaction of a molecule with a monoenergetic beam of soft X-rays[19]. E.s.c.a. is inherently sensitive to the surface because of the very short mean free path of electrons

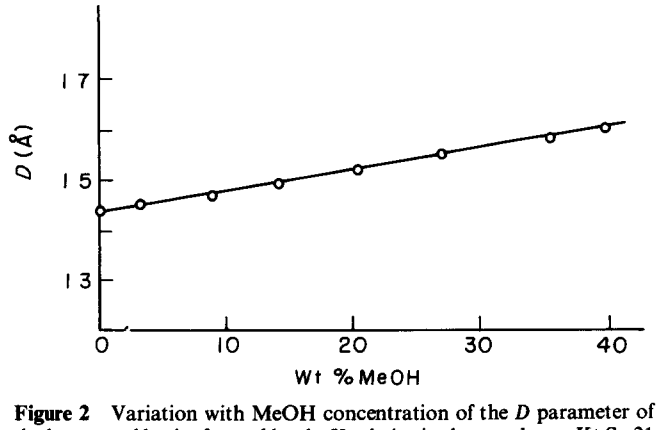

Figure 2 Variation with MeOH concentration of the D parameter of the hexagonal lattice formed by the Kt chains in the copolymer Kt.Sa 21

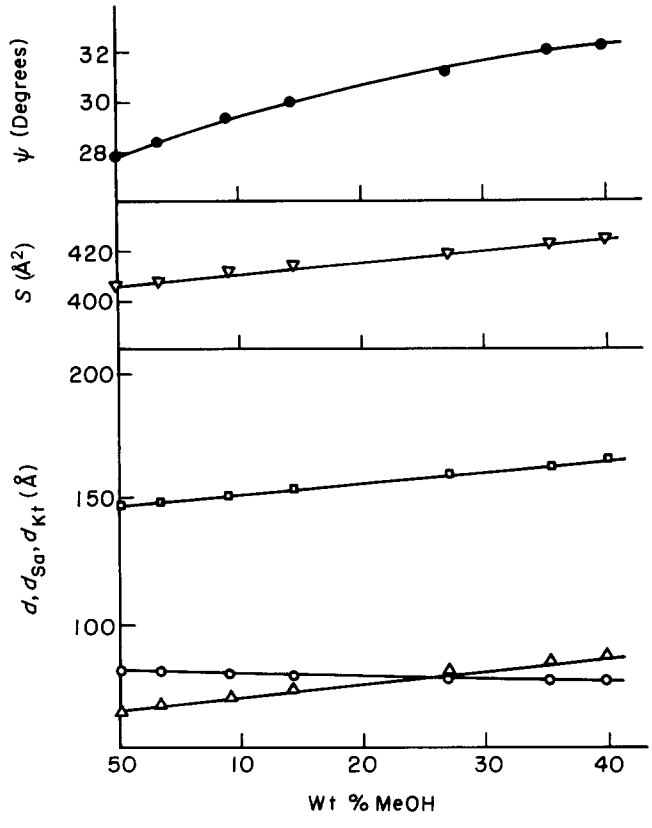

Figure 3 Variation with MeOH concentration of the lamellar structure parameters for the copolymer Kt.Sa 21. The symbols are as follows: (□) d, intersheet spacing; (○) d_{Kt}, Kt layer thickness; (△), d_{Sa}, Sa layer thickness; S, specific surface; ψ, angle of tilt of the Kt chains

Table 2 Lamellar structure parameters for dry copolymers

Sample	25	21	26
Wt% Kt	27.7	57.4	74.4
d (Å)	224	147	121
d_{Kt} (Å)	59	82	88
d_{Sa} (Å)	165	65	33
S (Å²)	563	406	374
ψ (deg)	50.4	27.8	16.3

(<100 Å) and its strong dependence on kinetic energy[19,20]. Based upon previous knowledge of the electron mean free paths of photoemitted electrons from C_{1s}, N_{1s}, O_{1s} and F_{1s} core levels[12,20-22], it may be assumed that in samples studied the maximum effective sampling depth is about 35 Å, i.e. about 95% of the signal intensity comes from the outermost ~35 Å.

Data used for the determination of the polymer surface composition were the relative binding energies (*BE*) and the peak intensities corresponding to direct photoionization of the core levels.

Binding energies of photoemitted electrons allow one to identify atoms present in the sample and their chemical environment. Peak area ratios allow one to determine the number ratio of these atoms.

For a bulk homogeneous sample of thickness essentially infinite compared with the typical electron mean free paths, the intensity of the elastic peak for photoemission from core level i may be expressed as[23,24]:

$$I_i=F_iK_iN_i\alpha_i\lambda_i \quad (3)$$

with λ_i the mean free path of electrons photoemitted from the core level i, α_i the cross-section for photoionization in a given shell (i) for a given atom and for a given X-ray photoelectron energy, N_i the number of atoms per unit volume on which the core level i is located, F_i the X-ray flux irradiating the sample, and K_i a spectrometer factor.

In a given sample, the intensity ratio of elastic peaks arising from two different core levels i and j is expressed as:

$$\frac{I_i}{I_j}=\frac{K_i\alpha_i\lambda_i N_i}{K_j\alpha_j\lambda_j N_j}=R\frac{N_i}{N_j} \quad (4)$$

For two given atoms the R factor was determined on model compounds of known stoichiometries. Results are given in *Table 3*.

Homopolymers. The component homopolymers Kt and Sa were first studied in order to establish a basis for the interpretation of the diblock copolymer data.

(a) *Kt homopolymers.* E.s.c.a. spectra of Kt display four signals for the C_{1s}, N_{1s}, O_{1s} and F_{1s} levels. The N_{1s}, O_{1s} and F_{1s} lines consist of a single peak respectively centred at 399.3 eV, 530.9 eV and 688.0 eV referenced to hydrocarbon C_{1s} at 285.0 eV. The C_{1s} line is broad and was assumed to be due to five different contributions as shown in the following formula:

Kt 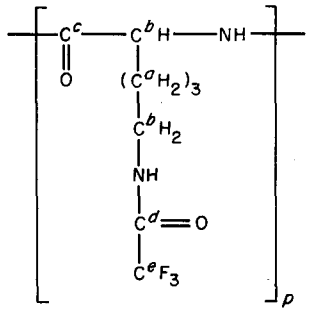 (5)

As the binding energy increases, the spectral lines expected were successively the signals of the aliphatic carbon (C^a), the carbon bonded to nitrogen (C^b), the carbonyl carbon pertaining to the main chain of the polypeptide (C^c), the carbonyl carbon pertaining to the side chain of the polypeptide (C^d) and at the highest binding energy the carbon bonded to three fluorines (C^e).

The shift in binding energy of the C atom adjacent to CF_3 was ascribed to the secondary substituent effect of fluorine. Evidence for this effect was given by Clark and coworkers[21,25]. They reported a secondary shift of 0.7 eV for carbon substituted with one fluorine and approximately 1.3 eV for carbon substituted with more than one fluorine.

Computer analysis of the C_{1s} spectra of Kt was performed with five peaks of equal width, leaving the peak positions and intensities to be adjusted. A typical result for the C_{1s} peak analysis is given in *Figure 4*. The

Table 3 Instrumental sensitivity ratios R at fixed operating conditions

Core level ratios	Peak area ratios
C_{1s}/O_{1s}	0.35
C_{1s}/N_{1s}	0.52
C_{1s}/F_{1s}	0.21

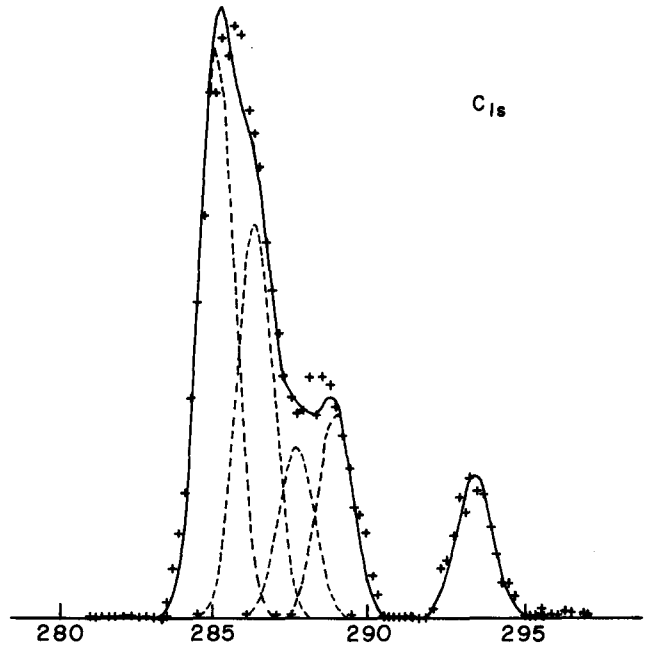

Figure 4 C_{1s} core level spectra for the Kt homopolymer cast from MeOH. Points: experimental data after background removal. Broken curves: calculated curves for the various components. Full curves: fitted envelope

Table 4 Contributions to C_{1s} signals in Kt and Sa homopolymers

		BE (eV)	
C_{1s} type		Kt	Sa
C^a	$(CH_2)_n$	285.0	
C^b	C–N	286.3	286.5
C^c	C=O	287.7	287.8
C^d	C=O	288.9	
C^e	CF_3	293.0	

experimental binding energies are listed in *Table 4*. They are in close agreement with the values given in the literature.

The stoichiometry of the Kt homopolymer was calculated by two independent methods. The first is based on the relative peak areas of the total C_{1s}, N_{1s}, O_{1s} and F_{1s} peaks. The second method is based on the relative intensities of the signals of the C_{1s} components. The values obtained from the two independent means are in good agreement with one other and with the theoretically expected stoichiometry.

(b) *Sa homopolymers.* The e.s.c.a. spectra of the Sa component displays three signals corresponding to the C_{1s}, N_{1s} and O_{1s} levels. The O_{1s} and N_{1s} lines were fitted with a single peak respectively centred at 399.4 eV and 530.7 eV referenced to aliphatic carbon. The C_{1s} line was assumed to contain two different contributions as shown in the following formula:

Sa 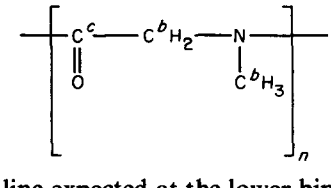 (6)

The spectral line expected at the lower binding energy was the signal of carbons bonded to nitrogen (C^b); the

other spectral line expected was the signal of the carbonyl carbon (C^c). Binding energy values of the structural features pertaining to Sa are given in *Table 4*. Atoms with the same electronic environment exist in the Kt and Sa components and the same relative binding energies are obtained within experimental error.

The Sa stoichiometry was calculated in the same way as for the Kt homopolymer. The result was consistent with the theoretical predictions.

Block copolymers. Three block copolymers with the same Kt block and different Sa content were studied (*Table 1*). For each copolymer type an example of the e.s.c.a. spectra obtained is shown in *Figure 5*.

Spectra of the Kt.Sa copolymers are the superposition of the Kt and Sa spectra described above and thereby resemble that of the Kt homopolymer. The relative binding energies are identical.

The C^a_{1s}, C^d_{1s}, C^e_{1s} and F_{1s} signals arise from the single Kt component. The C^b_{1s}, C^c_{1s}, N_{1s} and O_{1s} signals arise from both the components Kt and Sa. *Figure 5* shows that, for a given value of the C^a_{1s} peak area, the areas of the C^b_{1s}, C^c_{1s}, N_{1s} and O_{1s} signals decrease on passing from the copolymer Kt.Sa 25 to the copolymer Kt.Sa 21 and then to the copolymer Kt.Sa 26, indicating that the Kt concentration at the copolymer surface increases as the whole Kt content in the copolymer increases.

The composition of the copolymer surfaces was determined in two independent ways. In the first way we have compared the peak area ratios C_{1s}/F_{1s}, O_{1s}/F_{1s} and N_{1s}/F_{1s} for the copolymers and the Kt homopolymer. In the second way we have compared the peak area ratios C^b_{1s}/C^a_{1s} and C^c_{1s}/C^a_{1s} for the copolymers and the Kt homopolymer. Results obtained by these two means are in good agreement. They are listed in *Table 5*.

It is apparent that for copolymers Kt.Sa 25 and Kt.Sa 21, there is a significant excess of Kt at the surface compared to the bulk. For Kt.Sa 26, with the highest bulk content in Kt, the same composition is found at the surface.

Kt being the hydrophobic block in the copolymers studied, the enhancement of this block at the surface of

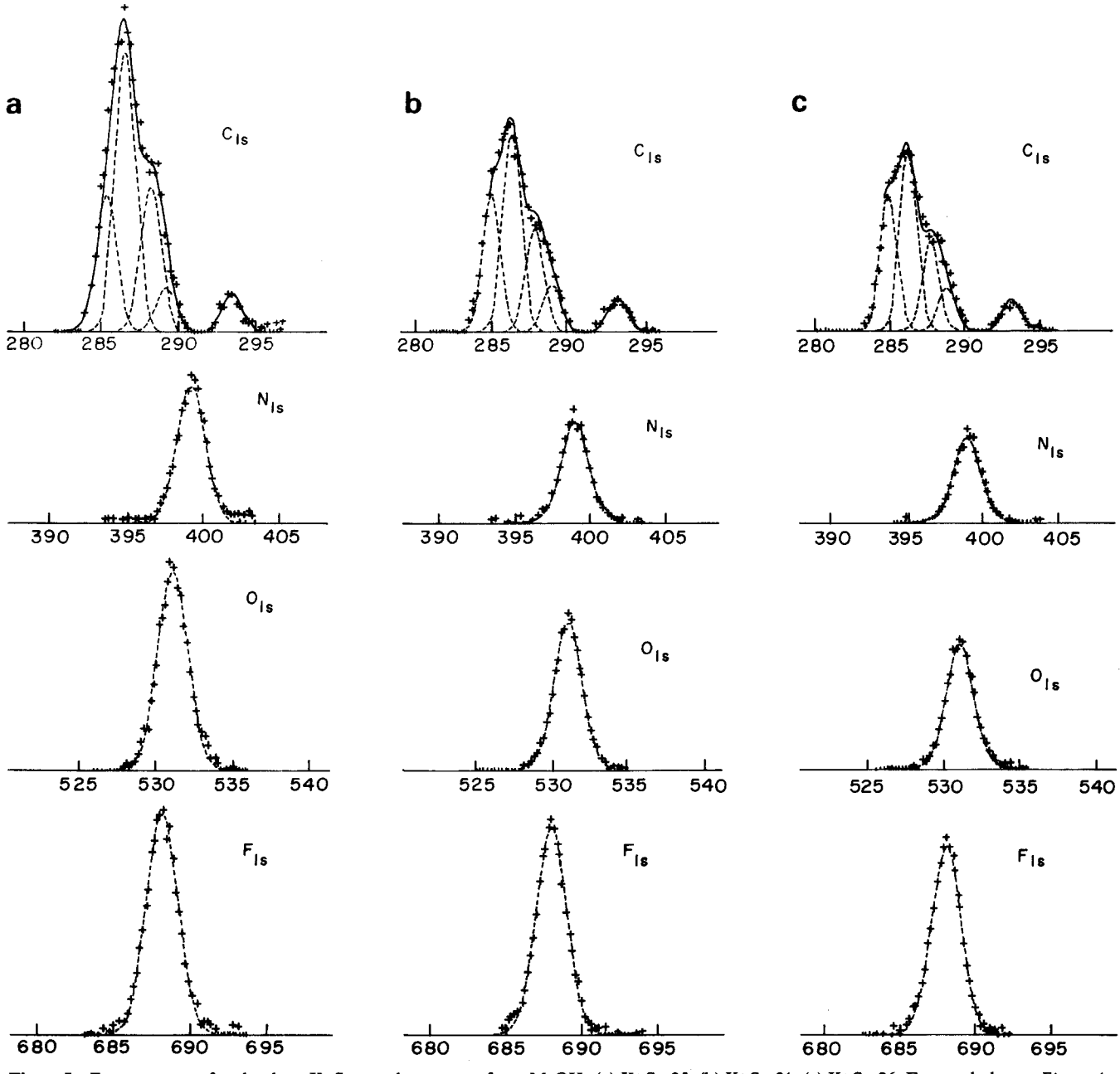

Figure 5 E.s.c.a. spectra for the three Kt.Sa copolymers cast from MeOH: (a) Kt.Sa 25, (b) Kt.Sa 21, (c) Kt.Sa 26. For symbols, see *Figure 4*

the copolymer allows a decrease in the surface free energy. Results concerning the composition in the top 35 Å give important indications with regard to the structure of the copolymer surface.

At the surface, the layers forming the lamellar structure of copolymers may be assumed parallel to the air–polymer interface or tilted on this interface.

If the layers are assumed parallel to the air–polymer interface, the surface excess of Kt found experimentally for the copolymers Kt.Sa 25 and Kt.Sa 26 implies that the Kt component is localized in the overlayer.

The Kt layer thicknesses determined by X-ray diffraction (*Table 2*) are significantly larger than the effective sampling depth for the three copolymers studied. For these copolymers only the signal arising from the Kt component would be observed. Data in *Table 5* show the presence of both components in the depth probed by e.s.c.a. These results clearly indicate that the Kt and Sa layers of the copolymers are not parallel to the surface.

Therefore a model of the surface structure of Kt.Sa copolymers was retained in which the Kt and Sa layers are perpendicular to the air–polymer interface.

In *Figure 6* is plotted the surface excess of Kt *versus* the Kt content of the bulk.

Table 5 and *Figure 6* indicate that the greatest surface enhancement in Kt is exhibited by the copolymer Kt.Sa 25 containing the least amount of Kt. The slope of the curve in *Figure 6* shows that the surface excess in Kt is more sensitive to variations in the bulk composition for copolymers containing less than about 20 mol% Kt.

Therefore it seems that molecular rearrangement providing an excess of Kt at the copolymer surface is easier when the molecular weight of the Sa block is high compared with the molecular weight of the Kt block.

Depth profiling and surface topography

All the results given above have been obtained by analysing the photoemitted electrons normal to the surface of the sample under investigation. With this experimental arrangement the effective sampling depth is maximized (~35 Å).

Table 5 Surface compositions for the three Kt.Sa copolymers

	Mol% Kt	
Sample	Bulk	Surface
25	10.9	34.8
21	30.0	45.2
26	48.0	47.4

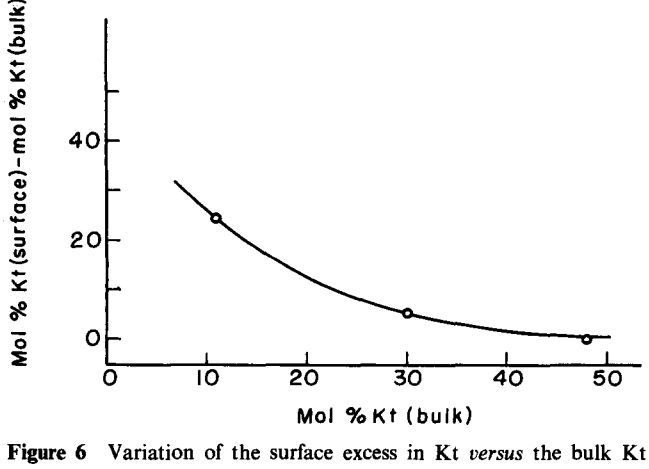

Figure 6 Variation of the surface excess in Kt *versus* the bulk Kt content

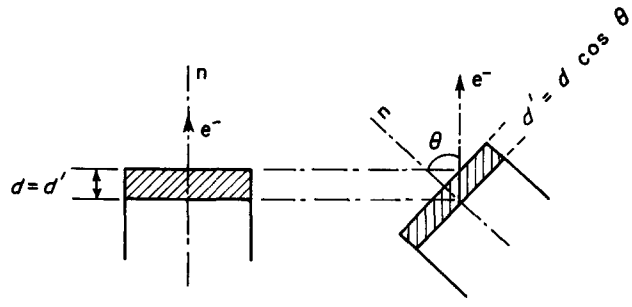

Figure 7 Variation of the effective sampling depth d' as a function of the electron take-off angle θ

The effective sampling depth can be controllably decreased by rotating the sample relative to the fixed-position energy analyser (*Figure 7*). The take-off angle θ, defined as the angle between the normals to the sample surface and to the slits in the analyser, is then increased. The decrease of the effective sampling depth (d') allows for depth profiling the composition of the upper 35 Å to yield insight into the molecular organization at the top surface and the surface topography[6,20,23]. Spectra were recorded at take-off angles θ ranging from 0 to 75° to achieve effective sampling depths from ~35 Å to ~9 Å.

Figure 8 displays the e.s.c.a. spectra for copolymer Kt.Sa 25 recorded at three take-off angles: $\theta=0°$, $d'\sim35$ Å; $\theta=45°$, $d'\sim25$ Å; $\theta=75°$, $d'\sim9$ Å.

For a given value of the C^a_{1s} peak area, the areas of the C^b_{1s}, C^c_{1s}, N_{1s} and O_{1s} peaks decrease when going to higher take-off angles. This variation indicates that the Kt content of the copolymer increases as the outermost surface is reached.

The compositions at various take-off angles θ were calculated for the three copolymers studied. The variation of the Kt content of the surface with θ is shown in *Figure 9*. As can be seen, the Kt content of the surface increases with the take-off angle θ for the three copolymers studied.

As the take-off angle θ increases from 0 to 75°:

(a) the Kt content of the Kt.Sa 25 surface increases from 34.8 to 58 mol%,

(b) the Kt content of the Kt.Sa 21 surface increases from 45.2 to 60 mol%, and

(c) the Kt content of the Kt.Sa 26 surface increases from 47.5 to 62 mol%.

The increase in the Kt content is similar (~15 mol%) for the copolymers Kt.Sa 21 and Kt.Sa 26, which have the same composition for $\theta=0°$.

The increase in the Kt content is larger (~25%) for the copolymer Kt.Sa 25, which has the smallest Kt content for $\theta=0°$. For the three copolymers studied, the Kt content of the surface tends to a value near to 60 mol% as the outermost surface is approached.

The increase in the Kt content as the effective sampling depth d' decreases may be explained by assuming that the Kt domains are slightly above the Sa domains at the copolymer surface (*Figure 10*).

The pre-eminence of the hydrophobic block at copolymer surfaces was shown on replication electron micrographs for polystyrene–poly(ethylene oxide) AB and BAB copolymers[26] and for copolymers with a central polybutadiene block and two polypeptide blocks[17,27]. Thomas and coworkers proposed a model similar to that

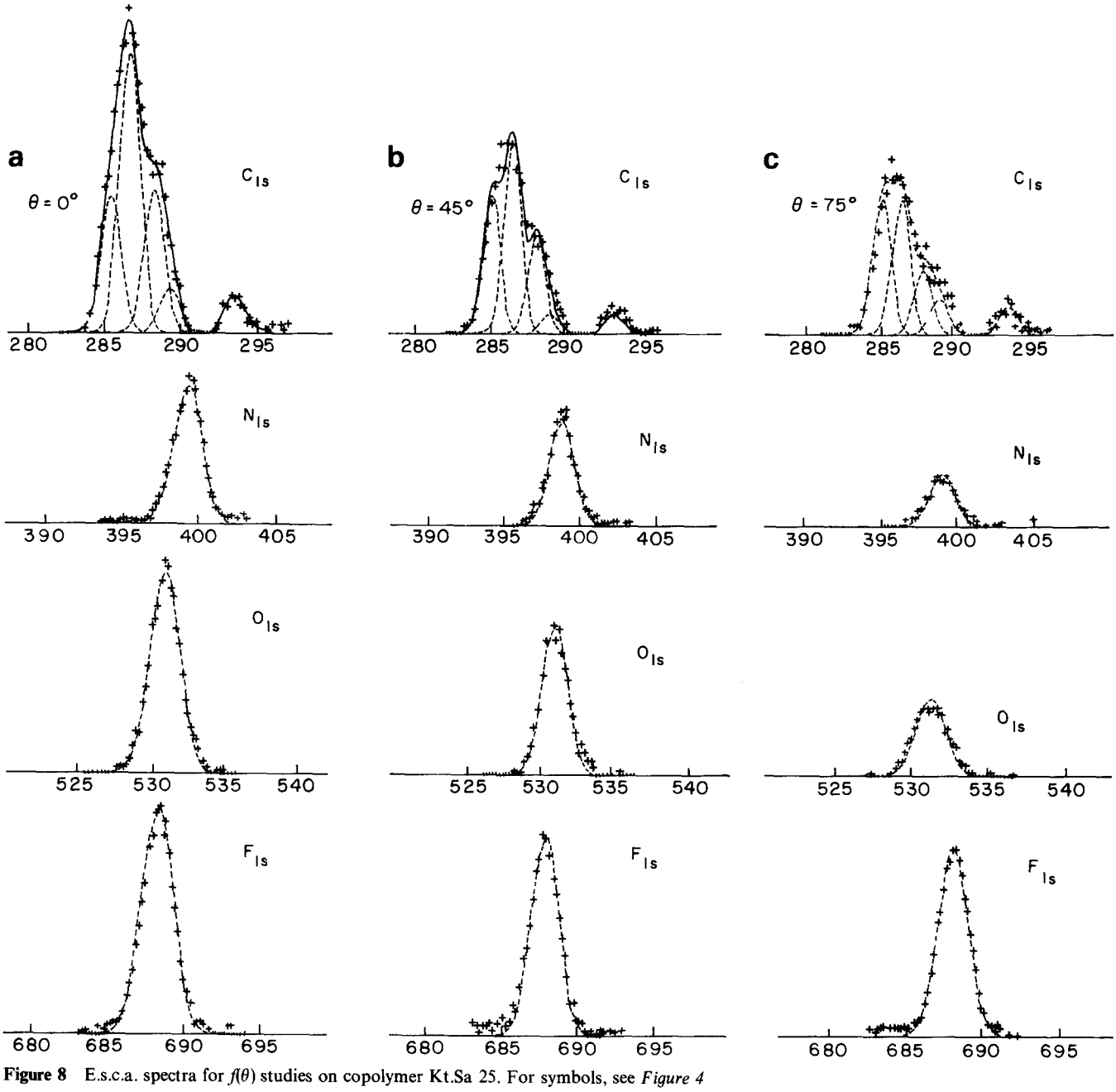

Figure 8 E.s.c.a. spectra for $f(\theta)$ studies on copolymer Kt.Sa 25. For symbols, see *Figure 4*

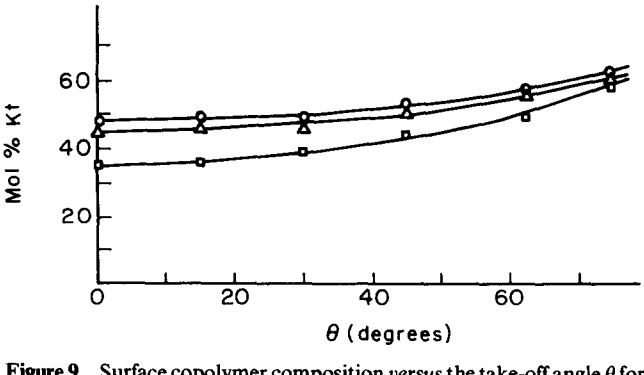

Figure 9 Surface copolymer composition *versus* the take-off angle θ for the three copolymers studied: □, Kt.Sa 25; △, Kt.Sa 21; ○, Kt.Sa 26

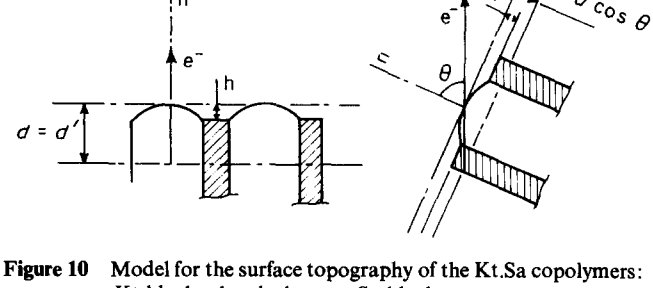

Figure 10 Model for the surface topography of the Kt.Sa copolymers: open areas, Kt blocks; hatched areas, Sa blocks

illustrated in *Figure 10* for the topography of block copolymers containing blocks of polystyrene and poly(ethylene oxide)[9,10].

CONCLUSIONS

Films of block Kt.Sa copolymers cast from MeOH, a mutual solvent of the two blocks, have been studied by e.s.c.a.

E.s.c.a. analysis of the top surface layer of the films some 35 Å thick has revealed the tendency of the hydrophobic Kt blocks to reside preferentially at the surface of the copolymers. The rearrangement of the Kt blocks at the surface is easier in copolymers with low Kt content. It does not occur for copolymers with Kt contents higher than about 45 mol%. E.s.c.a. analysis of surface layers with thicknesses in the range 35 to 9 Å has shown that the Kt content of the copolymer surface increases as the air–copolymer interface is approached. At the outermost surface the Kt content of the copolymer attains values close to 60 mol%.

X-ray diffraction studies of Kt.Sa copolymers in concentrated solution in MeOH and in the dry state have shown that they exhibit a lamellar structure formed by the superposition of layers containing alternately Kt blocks and Sa blocks.

From these experimental results a surface model is proposed in which the lamellar structure of the Kt.Sa copolymers is perpendicular to the air–polymer interface and the Kt component is raised above the Sa component.

Similar studies are now in progress on various block copolymers with the aim of determining the influence of the nature of the blocks, the solvent and the copolymer structure on the surface composition.

Contact angle measurements will soon be undertaken to evaluate the surface free energy of the block copolymers. It is hoped that correlation between the surface free energy data, e.s.c.a. and X-ray diffraction results will allow a better understanding of the block copolymer behaviour at a surface.

ACKNOWLEDGEMENTS

We wish to thank J. C. Auchet for his assistance in the adjustment of the computer program.

REFERENCES

1 Okano, T., Nishiyama, S., Shinomara, I., Akaike, T., Sakurai, Y., Kataoka, K. and Tsuruta, T. *J. Biomed. Mater. Res.* 1981, **15**, 393
2 Shimada, M., Miyahara, M., Tahara, H., Shinohara, I., Okano, T., Kataoka, K. and Sakurai, Y. *Polym. J.* 1983, **15**, 649
3 Yui, N., Tanaka, J., Sanvi, K. and Ogata, N. *Makromol. Chem.* 1984, **185**, 2259
4 Sasaki, T., Ratner, B. D. and Hoffman, A. S. *ACS Symp. Ser.* 71, Hydrogels for Medical and Related Applications (Ed. J. D. Andrade), American Chemical Society, Washington, 1976, p. 283
5 Sakurai, Y., Akaike, T., Kataoka, K. and Okano, T. 'Biomedical Polymers', Academic Press, New York, 1980
6 Clark, D. T. 'Advances in Polymer Science' (Eds. H. J. Canton *et al.*), Springer-Verlag, Berlin, 1977, pp. 24–126
7 Clark, D. T. in 'Polymer Surfaces' (Eds. D. T. Clark and W. J. Feast), Wiley, London, 1978, Ch. 16, p. 344
8 Clark, D. T. 'Structural Studies of Macromolecules by Spectroscopic Methods', (Ed. K. J. Ivin), Wiley, London, 1978, Ch. 9
9 Thomas, H. R. and O'Malley, J. J. *Macromolecules* 1979, **12**, 323
10 Thomas, H. R. and Lee, G. M. *Macromolecules* 1979, **12**, 996
11 Thomas, H. R. and O'Malley, J. J. *Macromolecules* 1981, **14**, 1376
12 Clark, D. T., Peeling, J. and O'Malley, J. J. *J. Polym. Sci., Polym. Chem. Edn.* 1976, **14**, 543
13 McGrath, J. E., Dwight, D. W., Riffle, J. S., Davidson, T. F., Webster, D. C. and Viswanathan, R. *Polym. Prepr. Am. Chem. Soc., Div. Polym. Chem.* 1979, **20**, 528
14 Pekala, R. W. and Merrill, E. W. *J. Colloid. Interface Sci.* 1984, **101**, 120
15 Inagaki, N. and Kishi, A. *J. Polym. Sci., Polym. Chem. Edn.* 1983, **21**, 1847
16 Inagaki, N., Kondo, S. and Murakami, T. *J. Appl. Polym. Sci.* 1984, **29**, 3595
17 Kugo, K., Hata, Y., Hayashi, T. and Nakajima, A. *Polym. J.* 1982, **14**, 401
18 Douy, A. and Gallot, B. *Polymer* submitted
19 Siegbahn, K., Nordling, C., Fahlman, A., Nordberg, R., Hamrin, K., Hedman, J., Johansson, G., Berkmark, T., Karlsson, S. E., Lindgren, I. and Lindberg, B. in 'ESCA, Atomic, Molecular and Solid Structure Studied by Means of Electron Spectroscopy', Almquist and Wiksells, Uppsala, 1967
20 Clark, D. T. and Thomas, H. R. *J. Polym. Sci., Polym. Chem. Edn.* 1977, **15**, 2843
21 Clark, D. T. and Shuttleworth, D. *J. Polym. Sci., Polym. Chem. Edn.* 1978, **167**, 1093
22 Tracey, J. C. in 'Electron Emission Spectroscopy', (Ed. W. Dekeyser), Reidel, Dordrecht, 1973, p. 295
23 Fadley, C. S., Baird, R. J., Siekhaus, W., Novakov, T. and Biegstrom, S. A. L. *J. Electron Spectrosc.* 1974, **4**, 93
24 Carlson, T. A. and McGuire, G. E. *J. Electron Spectrosc.* 1972, **1**, 161
25 Clark, D. T., Feast, W. J., Kilcast, D. and Musgrave, W. K. R. *J. Polym. Sci., Polym. Chem. Edn.* 1973, **11**, 389
26 Crystal, R. G., Erhardt, P. F. and O'Malley, J. J. in 'Block Copolymers', (Ed. S. L. Aggarval), Plenum Press, New York, 1970, p. 179
27 Kugo, K., Marashima, M., Hayashi, T. and Nakajima, A. *Polym. J.* 1983, **15**, 267